A Hardware-friendly Neuromorphic Spiking Neural Network for Frequency Detection and Fine Texture Decoding

Michele Mastella[1,2], *Student Member*, *IEEE*, Elisabetta Chicca[1,2], *Senior Member*, *IEEE*

***Abstract*—Humans can distinguish fabrics by their textures, even when they are finer than the density of tactile sensors. Evidence suggests that this ability is produced by the nervous system using an active touch strategy. When the finger slides over a texture, the nervous system converts the texture's spatial period into an equivalent spiking frequency. Many studies focused on modeling the biological encoding part that translates the spatial frequency into a temporal spiking frequency, but few explored the decoding part. In this work, we propose a novel approach based on a spiking neural network able to detect the frequency of an input signal. Inspired by biological evidence, our architecture detects the range in which the encoded frequency dwells and could therefore decode the texture's spatial period. The network has been designed to be composed of existing neuromorphic spiking primitives. This property enables a straightforward implementation on integrated silicon circuits, allowing the texture decoding at the edge of the sensor.**

***Index Terms*—Spiking Neural Network, Phase-Locked Loop, texture, active touch, neuromorphic**

I. Introduction

Humans find in touch a great ally. This sense is fundamental for our daily life due to the many abilities it incorporates. The most known ones are shape detection, texture recognition, slip detection, grip control, and vibration detection [1]. To be able to create such a colorful variety of skills, the human body employs many different types of sensors embedded in the skin (called mechanoreceptors). Recent studies suggest that these abilities are enabled by a complex synergy between the different mechanoreceptors [1]. One of the examples of this synergy comes from texture recognition. There is evidence, coming from neuroscience experiments [2], that humans can perceive textures in two different ways. When the texture is coarse, a special type of mechanoreceptors, the slow adapting ones (SA1), encodes it. On the other hand, when the texture is finer than the skin's sensors density, another mechanism takes place: by sliding the finger over the texture, humans induce vibration on the skin [3]. This signal is perceived by some special mechanoreceptors called Pacinian corpuscles [4], sensible to high-frequency vibration [5], [6]. It has been demonstrated that the Pacinian afferents exhibit a response phase-locked with the input frequency when stimulated with a periodic vibration [7]. The specific periodic vibrations generated by the skin, when slid on different materials, help human distinguishing between fabrics. For example, the periodic vibration generated by nylon, stretch denim, and silk jacquard is shown in [2]. Based on this experimental evidence, several works exploited the concept that texture recognition relies on the mechanoreceptors' spatiotemporal behavior [8]–[10]. In [11]–[14], the authors propose the existence of a Spiking Phase-Locked Loop (sPLL) structure (a neural version of the Phase-Locked Loop, a quite popular circuit in electronics [15]) in the mouse's nervous system. The structure is able to decode touch information using the periodic spiking input. Starting from the idea that the brain employs sPLLs for touch, we designed a full neuromorphic chain and demonstrated its properties in simulations. The proposed architecture can encode and decode textures when they are slid on the skin. In this paper, we present the network's working principle and preliminary results. The proposed system consists of elementary blocks which have well established analog circuit implementations [16], therefore it is suitable for the design of a compact silicon realization. Such a realization would fully exploit the low-latency and compactness for seamless integration in prosthetic systems and robotics.

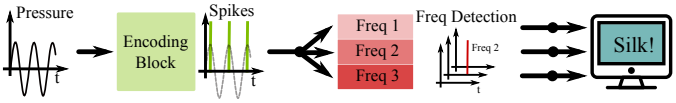

Fig. 1. Graphical representation of the designed network. The structure is composed of different stages: the first one is an encoding block, responsible for converting periodic analog signals into spikes, phase-locked with the periodicity of the stimulus. The second part is the frequency detection network, divided into several parallel blocks that transmit spikes when the stimulus' frequency is near to their characteristic one. Depending on which block spikes when a texture is presented, and knowing the characteristic frequency of each material, we can deduce which fabric was slid.

II. Methods

The proposed architecture has been designed to detect the signal oscillations coming from a tactile sensor. These oscillations, induced by materials sliding over the sensor, can be used as the basis for texture classification tasks. The underlying mechanism is simple: as observed in the Introduction, when we slide a texture on a pressure sensor, the latter generates a periodic analog signal. The sensor's output produces a

This work has been supported by the EU H2020 project Neutouch grant No. 813713. The authors would like to acknowledge the financial support of the CogniGron research center and the Ubbo Emmius Funds (Univ. of Groningen).

Affiliations: [1] Bio-Inspired Circuits and Systems (BICS) Lab. Zernike Institute for Advanced Materials (Zernike Inst Adv Mat), University of Groningen (Univ Groningen), Nijenborgh 4, NL-9747 AG Groningen, Netherlands.
[2] CogniGron (Groningen Cognitive Systems and Materials Center), University of Groningen (Univ Groningen), Nijenborgh 4, NL-9747 AG Groningen, Netherlands.

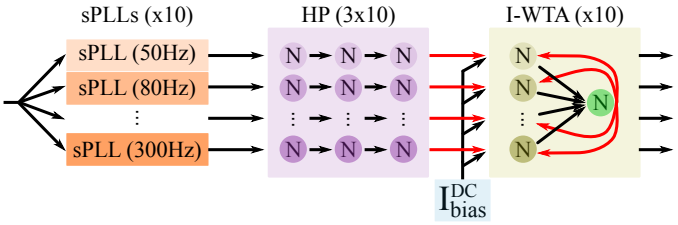

Fig. 2. Frequency Detection Network. The structure is divided into 10 lines able to decode 10 different frequency ranges. The first part of each line is composed of a sPLL that, depending on the input current provided, is sensible to specific frequencies. Then for each line we have three layers of simple Leaky Integrate-and-Fire (LIF) neurons that act as spiking High Pass Filter (HP), and a Inverted Winner-Take-All (I-WTA) network with a fixed bias input current I^{DC}_{bias}. The output of this last part encodes the range in which the input frequency dwells. The red lines represent inhibitory connections, while the black ones represent excitatory connections.

specific characteristic frequency that distinguishes the applied texture. The network can detect this characteristic frequency and therefore recognize the texture. The first step in the acquisition chain, visible in Figure 1, is the encoding part. The encoding block is responsible for detecting peaks in the pressure signal and converting them into spikes. In this work, to test the architecture, we directly synthesized the spikes with specific frequencies, leading to a simulated encoding block's output. Once the stimulus is encoded into spikes, the signal is fed into the Frequency Detection block, represented in Figure 1 by several red blocks receiving the same input stimulus from the encoding block. Each of these red blocks has a different characteristic frequency. When an input signal is close to said frequency (it is into its sensitivity range), the correct Frequency block communicates it to the output. Depending on which block is activated, we can therefore understand which texture has been presented and, from this, decode which material it was. The internal structure of the Frequency Detection block is presented in detail in Figure 2 and explained in the following Subsections. It is composed of several sPLLs in parallel, followed by three layers of neurons, composing the High Pass Filter (HP) block, and a further layer of neurons, implementing a soft Inverted Winner-Take-All (I-WTA) computation.

A. Spiking Phase-Locked Loop

The first block is the sPLL, responsible of sorting the different frequencies. The structure, similar in concept to the one in [11], is composed of a Time Difference Encoder (TDE) [17]–[20] and a Current Controlled Oscillator (CCO). These two elements are closed in a negative loop, like in Figure 3.

1) Current Controlled Oscillator: The single neuron, represented in Figure 3 as CCO, is a Leaky Integrate-and-Fire (LIF) neuron [21]. This element is composed by two parts: a capacitor C_{mem} and a conductance G_{mem}, equipped with a negative feedback. When a current is fed into the element, the voltage V_{mem} over the capacitance increases. Once reached a threshold, the negative feedback resets the said voltage. The circuit then generates a spike and starts again charging the capacitance. This results in an element that has a spiking rate directly related to the current fed into its membrane

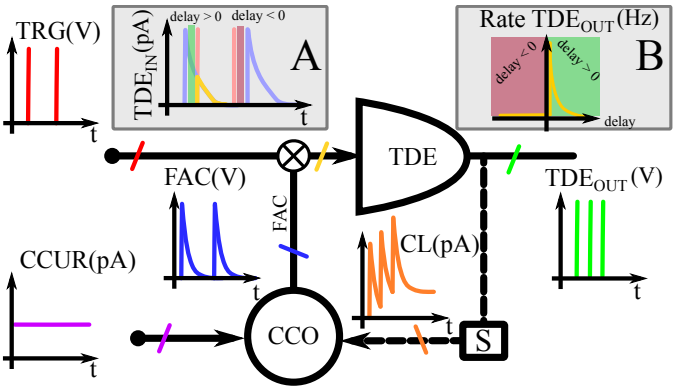

Fig. 3. The Spiking Phase-Locked Loop (sPLL)'s block diagram. This computational module is composed of a Time Difference Encoder (TDE) and a Current Controlled Oscillator (CCO). The first consists of a multiplier unit and a LIF neuron. The multiplier generates a current from the two inputs and injects it into the neuron. The CCO is also implemented with a simple LIF neuron, which is translating its input current into an output firing rate. The CCO's input current is composed by two contributions: a constant current (CCUR, violet line) and a Closed-Loop current (CL, orange line). The first one defines the CCO's intrinsic spike rate, while the latter one transmits the spikes from the TDE_{OUT}'s LIF, after converting them to current. Regarding the TDE, the two input signals (TRG, red line, and FAC, blue line) are respectively connected to the spikes coming from the sensor, and the spikes coming from the CCO. For each CCO's spike, its output exhibits an exponentially decaying function. By multiplying the FAC and TRG signals, we are able to compute the time proximity between them. The result of the computation elicits a current response TDE_{IN} that depends on the time TRG arrives after FAC, as visible in Figure A. This current is then fed into the TDE's LIF neuron. Its output is represented by TDE_{OUT}. Given its nature, its spiking activity directly depends on the FAC and TRG time proximity, as visible in Figure B. The TDE_{OUT}'s response is then directly wired to the neuron's input in a closed-loop fashion.

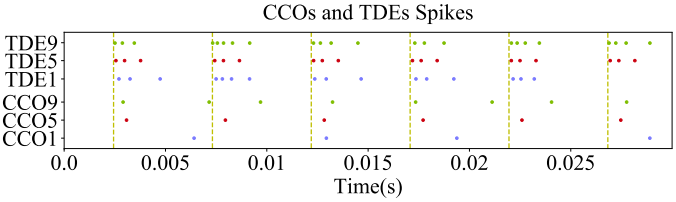

Fig. 4. A raster plot shows an example of three different sPLL's behaviors. The vertical yellow lines identify the time of each input spike. The spike's phases, coming from each of the CCO, is compared with the input signal phase. This happens for each input spike, and the result of the TDE's output is a spike burst representing the phase proximity. Given the quite long τ_{LIF} (around 10 ms), when the input rate is fast (in this case 205 Hz), the TDE output spike is influenced by the previous occurrences. The three CCOs (blue, red, and green) have different constant current inputs (CCUR) that make them spike differently. One of them (the red one) is close enough to the input frequency to lock.

capacitance. By feeding the element with different currents, we are therefore able to change its spiking frequency. This solution acts here as a CCO.

2) Time Difference Encoder: This block is able to encode time differences in spike rate. As visible in Figure 3, it's composed of a block that converts the multiplication between the two voltage inputs (FAC and TRG) into a current TDE_{IN} (the yellow line in Figure 3A), and by a neuron which receives this current. Being the latter a LIF neuron, it reacts with a spiking rate proportional to the TDE_{IN} current intensity. Every time a spike from the facilitatory node (FAC) reaches the TDE, it elicits an exponentially decaying response (the blue

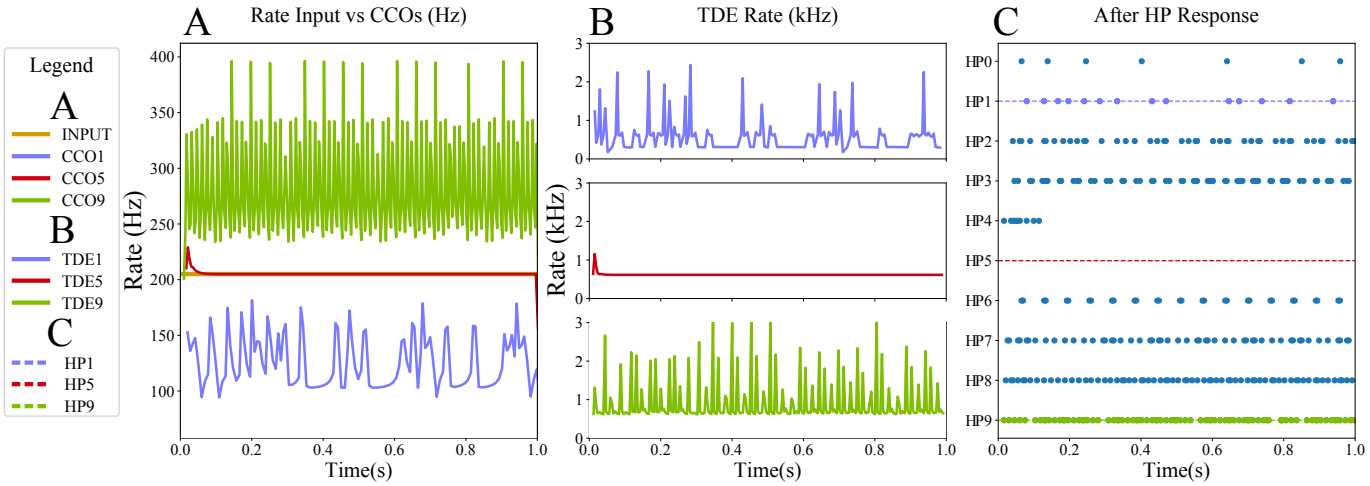

Fig. 5. An example of the network's underlying working principle. In Figure A, it's shown the instantaneous rate of 4 different elements. The straight yellow line at 205 Hz represents the frequency at which the input signal spikes. The CCO's spiking activity of three different lines is also plotted (Line 1 blue, Line 5 red, Line 9 green). Each of these CCOs, fed with a different current, has a different intrinsic frequency. The closed-loop tries to modify the phase difference between the input and the spiking neuron. The system reaches the locking if the CCO is close enough to the input frequency. For this example, we selected a low intrinsic frequency (Line 1, 80 Hz), an intermediate intrinsic frequency (Line 5, 230 Hz), and a high intrinsic frequency (Line 9, 300 Hz). Line 5 locks with the input while the others struggle to do it. In Figure B the three respective TDE's outputs are shown (response averaged over 3 samples). The locked one exhibits a low uniform frequency, while the other two have higher peaks. Figure C shows a raster plot of the HP neurons' output. The three lines shown in the previous two columns are here highlighted in the same colors. Line 1 and Line 9 have an output frequency given by their high peak activity in the TDE. Line 5's output is silent because its low frequency has been cut, Line4 shows a similar behavior, despite taking more time to reach it. The I-WTA selects the Line 5 as the winner, being the most inactive.

one in Figure 3) that is sensed by the multiplier. If during the FAC's decaying response, a spike from the trigger node (TRG) (the red one in Figure 3) reaches the multiplier, then the TDE produces a current proportional to the FAC's value at the TRG spike's time (this value is decreasing with the time distance between FAC and TRG spikes). This causes the TDE's LIF neuron to respond with a spike burst TDE_{OUT} (the green one in Figure 3), proportional in rate to the current TDE_{IN}, and therefore to the time proximity (Figure 3B). If the input signals are periodic, like in this case, then the TDE_{OUT} rate encodes the phase difference.

In Figure 4 we can see an example of the explained working principle. When the CCO emits a spike (we can see CCO1, CCO5, and CCO9), the TDE calculates the distance between this spike and the input spike (represented in the Figure with a dashed vertical yellow line). Due to the neuron's time constant, in some cases higher than the input spiking period ($\tau = C_{mem}R_{mem} = 10ms$), the result of the time difference's instantaneous calculation depends also on the recent TDE's activity.

3) Closed Loop: The architecture, composed of the two blocks previously explained, works as a PLL. This mechanism, well known in the frequency synthesis field [15], [22], relies on the CCO's ability to synchronize to the input's spike rate. The CL current (orange line in Figure 3), coming from the TDE, can increase the CCO's frequency, acting as a closed-loop in the following way: the higher is the phase difference between the two signals, the higher is the number of spikes in the TDE's burst. This response increases the CCO's spiking frequency. By changing said frequency, the loop modifies the phase difference between the CCO and the input spikes up to the point where the TDE's spiking activity is minimal, which is the optimal position. This can be seen in Figure 4 in the TDE5 line. The CCO5 is locked with the input stimulus and the TDE5 keeps spiking with a fixed pattern, which is the equilibrium point of the system to keep the two signal locked. This works only when the frequency difference between the two signals is small enough so that the loop can keep the phase error constant. If the frequency difference is too high, the phase difference between the input and the CCOs quickly accumulates and the sPLL is not fast enough to compensate it. This can be seen in Figure 4 where CCO1 and CCO9 have a different frequency concerning the input stimulus, and their TDEs have a heterogeneous response, given by the phase accumulation. Due to this effect, the time difference periodically changes from very high to very low. In the latter the TDE spikes with a frequency higher than 1 kHz. Therefore, on average, TDEs in unlocked situations exhibit more episodes of intense activity with respect to the locked situation. Figure 5B provides evidence of this behavior. The two lines that cannot lock have an irregular TDE activity, with peaks up to 3 kHz. Note that by changing the currents in input at CCO we can move upward or downward the system's sensitivity range.

B. High Pass Filter

In the sPLL block, we demonstrated that there is a dependence between the TDE_{OUT}'s spiking activity and the locking/not locking situation. This mechanism can be used to detect which PLL has the closest frequency concerning the input one (i.e. it can lock with it). To do so, we used three layers of LIF neurons with a feed-forward 1 to 1 connectivity pattern connected to the sPLLs (as visible in Figure 2 under HP). These neurons, thanks to their leaky part that constantly

discharge the neuron membrane, spike only when the input frequency is fast enough to charge the C_{mem} up to the neuron's threshold. This means that the neuron is insensible to the TDE's bursts when the burst's interspike interval is higher than $1\,\mathrm{ms}$. Considering the behavior explained previously, we are then filtering out the response of the PLL that is locked. The presence of three instances of the same neuron in series comes from the need to be sensitive only to frequencies higher than $1\,\mathrm{KHz}$ using components compatible with circuit implementations. We, therefore, repeated 3 times the same operation to ensure the HP's strength with the minimum number of components.

C. Inverted Winner Take All

The I-WTA represents the last part of the Frequency detection block. This block, composed of a layer of LIF neurons, receives an external constant current I_{bias}^{DC}, making all the neurons spike continuously. Each neuron is connected with one neuron from the HP layer through an inhibitory connection. This means that the more active HP neurons are inhibiting the corresponding I-WTA's neurons in a stronger way. All of the I-WTA's neurons are exciting a single global inhibition neuron. The spiking activity of this last element inhibits the I-WTA neurons permitting only the strongest one to spike. The neuron that has the highest spiking activity is selected as the winner.

III. Results

A. Single Frequency Experiment

The network presented in the Methods section has been simulated using Brian2 [23].

Figure 5 shows the details of the different signals inside the architecture during a simulation with only one input frequency ($205\,\mathrm{Hz}$). To simplify the visualization, in Figure 5A and 5B, we only plotted 3 out of the 10 lines in which the network is divided (specifically Line 1, Line 5, and Line 9). In Figure 5A, the spiking frequency of the three lines' CCOs is compared with the input's spiking frequency. Line 1 and Line 9's frequencies are not close enough to the input's frequency to achieve locking, while Line 5 is close enough to lock. Figure 5B shows the TDE_{out}'s spiking frequency. The two lines that are not able to lock exhibit a denser pattern of fast spikes (subsequent spikes, close in time). The line that is locked shows a very uniform low spike rate. In Figure 5C, we can see the scatter plot of all HP neurons. By filtering out the fast spikes, Line 5 has no spikes, while all the other 9 Lines still have spikes.

B. Sweeping Frequencies Experiment

In this experiment we generated different spiking frequencies, ranging from $0\,\mathrm{Hz}$ to $500\,\mathrm{Hz}$, to simulate what is observed in Pacini corpuscles, sensible to frequencies up to $800\,\mathrm{Hz}$ [7]. The HP's output was fed into a I-WTA. For each input frequency, we analyzed the I-WTA's spiking output and declared as the winner the neuron with the highest spike count. If due to the overall TDEs' low activity, more than one of I-WTA's neurons had the highest value, we considered that trial as failed.

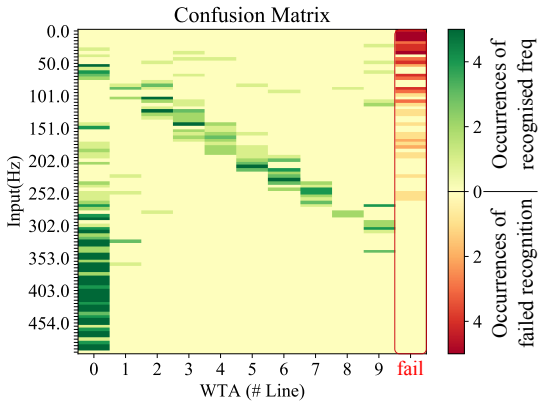

Fig. 6. The confusion matrix resulting from the inverted I-WTA stage. We generated a sample for each frequency, ranging from $0\,\mathrm{Hz}$ to $500\,\mathrm{Hz}$ with $1\,\mathrm{Hz}$ step. Each of these has been tested once, for 1 second each, on the structure, measuring which I-WTA neuron had a higher spiking rate, counting this as the winner. If more than one I-WTA neuron had the higher rate the algorithm counted it as fail (the last x-axis value in the plot). In the confusion matrix, the frequencies, represented on the y-axis, have been collected in bins of $5\,\mathrm{Hz}$ to increase visibility.

The result is shown in Figure 6, using a confusion matrix. Some conclusions can be drawn from these results. When the signal's frequency is lower than the lowest CCO intrinsic frequency, all the 10 TDEs are not stimulated enough to generate spikes. This keeps the whole system in an idle state and the I-WTA's neurons are driven only by the external input current. This results in a failed trial since all of the I-WTA's neurons spike synchronously. In the range between $50\,\mathrm{Hz}$ and $250\,\mathrm{Hz}$, the system works as expected: different PLLs lock with different frequency ranges and the I-WTA spikes correspondingly. The Line0 has the lowest input frequency from the CCO. This binds the TDE to receive spike bursts less often, making its spiking activity lower in frequency peaks and being filtered out by the HP block. For input frequencies higher than $250\,\mathrm{Hz}$, the system struggles to recognize the right frequency because of Line0's low activity, similar to one of the lines that locked to the frequency.

IV. Conclusions

In this work, we proposed a spiking neural network able to detect frequencies. The network is capable of distinguishing 10 different frequency ranges (from $50\,\mathrm{Hz}$ to $300\,\mathrm{Hz}$). The structure aims to explore the idea that PLL in the brain could be used for texture decoding [11]. Following studies will assess if this solution enables the detection of complex multiple frequency signals coming from fine texture, based on data provided by one sensor. This can relax the need for high-density distribution of sensors. Furthermore, the proposed structure is composed of building blocks that can be easily implemented in CMOS circuits. Examples of leaky integrate and fire neurons are abundant [16], [24] and a TDE circuit implementation has been already proposed [17]. Integrated neuromorphic circuits have the advantage to reduce power consumption and circuit footprint. This aspect is needed to integrate texture recognition at the edge of the sensor, for example in robots and prostheses.

REFERENCES

[1] H. P. Saal and S. J. Bensmaia, "Touch is a team effort: interplay of submodalities in cutaneous sensibility," *Trends in Neurosciences*, vol. 37, no. 12, pp. 689–697, 2014.

[2] A. I. Weber, H. P. Saal, J. D. Lieber, J.-W. Cheng, L. R. Manfredi, J. F. Dammann, and S. J. Bensmaia, "Spatial and temporal codes mediate the tactile perception of natural textures," *Proceedings of the National Academy of Sciences*, vol. 110, no. 42, pp. 17 107–17 112, 2013.

[3] M. Hollins and S. J. Bensmaïa, "The coding of roughness," *Canadian Journal of Experimental Psychology = Revue Canadienne De Psychologie Experimentale*, vol. 61, no. 3, pp. 184–195, 2007.

[4] A. Biswas, M. Manivannan, and M. A. Srinivasan, "Vibrotactile Sensitivity Threshold: Nonlinear Stochastic Mechanotransduction Model of the Pacinian Corpuscle," *IEEE Transactions on Haptics*, 2014.

[5] E. L. Mackevicius, M. D. Best, H. P. Saal, and S. J. Bensmaia, "Millisecond Precision Spike Timing Shapes Tactile Perception," *Journal of Neuroscience*, vol. 32, no. 44, pp. 15 309–15 317, 2012.

[6] C. M. Greenspon, K. R. McLellan, J. D. Lieber, and S. J. Bensmaia, "Effect of scanning speed on texture-elicited vibrations," *Journal of The Royal Society Interface*, vol. 17, no. 167, p. 20190892, 2020.

[7] M. A. Harvey, H. P. Saal, J. F. D. Iii, and S. J. Bensmaia, "Multiplexing Stimulus Information through Rate and Temporal Codes in Primate Somatosensory Cortex," *PLOS Biology*, vol. 11, no. 5, p. e1001558, 2013.

[8] C. M. Oddo, L. Beccai, J. Wessberg, H. B. Wasling, F. Mattioli, and M. C. Carrozza, "Roughness Encoding in Human and Biomimetic Artificial Touch: Spatiotemporal Frequency Modulation and Structural Anisotropy of Fingerprints," *Sensors*, vol. 11, no. 6, pp. 5596–5615, 2011.

[9] U. B. Rongala, A. Mazzoni, and C. M. Oddo, "Neuromorphic Artificial Touch for Categorization of Naturalistic Textures," *IEEE Transactions on Neural Networks and Learning Systems*, vol. 28, no. 4, pp. 819–829, 2017.

[10] M. Meier, G. Walck, R. Haschke, and H. J. Ritter, "Distinguishing sliding from slipping during object pushing," in *2016 IEEE/RSJ International Conference on Intelligent Robots and Systems (IROS)*, 2016, pp. 5579–5584.

[11] E. Ahissar, S. Haidarliu, and M. Zacksenhouse, "Decoding temporally encoded sensory input by cortical oscillations and thalamic phase comparators," *Proceedings of the National Academy of Sciences*, vol. 94, no. 21, pp. 11 633–11 638, 1997.

[12] E. Ahissar, "Neuronal phase-locked loops," US Patent 6 581 046B1, 2003, type: patentus.

[13] ——, "Temporal-Code to Rate-Code Conversion by Neuronal Phase-Locked Loops," *Neural Computation*, vol. 10, no. 3, pp. 597–650, 1998.

[14] E. Ahissar and A. Arieli, "Figuring Space by Time," *Neuron*, vol. 32, no. 2, pp. 185–201, Oct. 2001.

[15] Guan-Chyun Hsieh and J. C. Hung, "Phase-locked loop techniques. A survey," *IEEE Transactions on Industrial Electronics*, vol. 43, no. 6, pp. 609–615, 1996.

[16] E. Chicca, F. Stefanini, C. Bartolozzi, and G. Indiveri, "Neuromorphic electronic circuits for building autonomous cognitive systems," *Proceedings of the IEEE*, vol. 102, no. 9, pp. 1367–1388, 2014.

[17] M. B. Milde, O. J. N. Bertrand, H. Ramachandran, M. Egelhaaf, and E. Chicca, "Spiking Elementary Motion Detector in Neuromorphic Systems," *Neural Computation*, vol. 30, no. 9, pp. 2384–2417, 2018.

[18] G. V. D'Angelo, E. Janotte, T. Schoepe, J. O'Keeffe, M. Milde, E. Chicca, and C. Bartolozzi, "Event-based eccentric motion detection exploiting time difference encoding," *Frontiers in Neuroscience*, vol. 14, 2020.

[19] T. Schoepe, D. Gutierrez-Galan, J. P. Dominguez-Morales, A. Jimenez-Fernandez, A. Linares-Barranco, and E. Chicca, "Neuromorphic Sensory Integration for Combining Sound Source Localization and Collision Avoidance," in *2019 IEEE Biomedical Circuits and Systems Conference (BioCAS)*, 2019, pp. 1–4.

[20] D. Gutierrez-galan, T. Schoepe, J. P. Dominguez-Morales, A. Jimenez-Fernandez, E. Chicca, and A. Linares-Barranco, "An event-based, digital time difference encoder model implementation for neuromorphic systems," *TechRxiv*, Oct 2020 (Preprint).

[21] N. Brunel and M. C. W. van Rossum, "Quantitative investigations of electrical nerve excitation treated as polarization: Louis Lapicque 1907 · Translated by:," *Biological Cybernetics*, vol. 97, no. 5, pp. 341–349, 2007.

[22] P. Su and S. Pamarti, "Fractional-n Phase-Locked-Loop-Based Frequency Synthesis: A Tutorial," *IEEE Transactions on Circuits and Systems II: Express Briefs*, vol. 56, no. 12, pp. 881–885, 2009.

[23] M. Stimberg, R. Brette, and D. F. Goodman, "Brian 2, an intuitive and efficient neural simulator," *eLife*, vol. 8, p. e47314, 2019.

[24] M.-W. Kwon, M.-H. Baek, S. Hwang, K. Park, T. Jang, T. Kim, J. Lee, S. Cho, and B.-G. Park, "Integrate-and-fire neuron circuit using positive feedback field effect transistor for low power operation," *Journal of Applied Physics*, vol. 124, no. 15, p. 152107, 2018.